Inorg. Chem. **2004**, *43*, 4278–4288

Copper(II) Complexes of a Series of Alkoxy Diazine Ligands: Mononuclear, Dinuclear, and Tetranuclear Examples with Structural, Magnetic, and DFT Studies

Hilde Grove,[†] Timothy L. Kelly,[†] Laurence K. Thompson,*[,†] Liang Zhao,[†] Zhiqiang Xu,[†] Tareque S. M. Abedin,[†] David O. Miller,[†] Andrés E. Goeta,[‡] Claire Wilson,[§] and Judith A. K. Howard[‡]

Department of Chemistry, Memorial University, St. John's, Newfoundland A1B 3X7, Canada, Department of Chemistry, University of Durham, Durham DH1 3LE, U.K., and Department of Inorganic Chemistry, University of Nottingham, Nottingham NG7 2RD, U.K.

Received March 5, 2004

Picolyl hydrazide ligands have two potentially bridging functional groups (μ-O, μ-N–N) and consequently can exist in different coordination conformers, both of which form spin-coupled polynuclear coordination complexes, with quite different magnetic properties. The complex $[Cu_2(POAP\text{-}H)Br_3(H_2O)]$ (**1**) involves a μ-N–N bridge (Cu–N–N–Cu 150.6°) and exhibits quite strong antiferromagnetic coupling ($-2J = 246(1)$ cm^{-1}). $[Cu_2(PZOAPZ\text{-}H)Br_3(H_2O)_2]$ (**2**) has two Cu(II) centers bridged by an alkoxide group with a very large Cu–O–Cu angle of 141.7° but unexpectedly exhibits quite weak antiferromagnetic exchange ($-2J = 91.5$ cm^{-1}). This is much weaker than anticipated, despite direct overlap of the copper magnetic orbitals. Density functional calculations have been carried out on compound **2**, yielding a similar singlet–triplet splitting energy. Structural details are reported for $[Cu_2(POAP\text{-}H)Br_3(H_2O)]$ (**1**), $[Cu_2(PZOAPZ\text{-}H)Br_3(H_2O)_2]$ (**2**), $[Cu_2(PAOPF\text{-}2H)Br_2(DMSO)(H_2O)]\cdot H_2O$ (**3**), $[Cu_4(POMP\text{-}H))_4](NO_3)_4\cdot 2H_2O$ (**4**), and PPOCCO (**5**) (a picolyl hydrazide ligand with a terminal oxime group) and its mononuclear complexes $[Cu(PPOCCO\text{-}H)(NO_3)]$ (**6**) and $[Cu(PPOCCO\text{-}H)Cl]$ (**7**). Compound **1** ($C_{12}H_{13}Br_3Cu_2N_5O_4$) crystallizes in the monoclinic system, space group $P2_1/c$, with $a = 15.1465(3)$ Å, $b = 18.1848(12)$ Å, $c = 6.8557(5)$ Å, $\beta = 92.751(4)°$, and $Z = 4$. Compound **2** ($C_{10}H_{13}Br_3Cu_2N_7O_4$) crystallizes in the triclinic system, space group $P\bar{1}$, with $a = 9.14130(1)$ Å, $b = 10.4723(1)$ Å, $c = 10.9411(1)$ Å, $\alpha = 100.769(1)$, $\beta = 106.271(1)°$, $\gamma = 103.447(1)°$, and $Z = 2$. Compound **3** ($C_{23}H_{22}Br_2Cu_2N_7O_{5.5}S$) crystallizes in the monoclinic system, space group $P2_1/c$, with $a = 12.406(2)$ Å, $b = 22.157(3)$ Å, $c = 10.704(2)$ Å, $\beta = 106.21(1)°$, and $Z = 4$. Compound **4** ($C_{52}H_{48}Cu_4N_{20}O_{18}$) crystallizes in the monoclinic system, space group $P2_1/n$, with $a = 14.4439(6)$ Å, $b = 12.8079(5)$ Å, $c = 16.4240(7)$ Å, $\beta = 105.199(1)°$, and $Z = 4$. Compound **5** ($C_{15}H_{14}N_4O_2$) crystallizes in the orthorhombic system, space group $Pna2_1$, with $a = 7.834(3)$ Å, $b = 11.797(4)$ Å, $c = 15.281(3)$ Å, and $Z = 4$. Compound **6** ($C_{15}H_{13}CuN_5O_5$) crystallizes in the monoclinic system, space group $P2_1/c$, with $a = 8.2818(9)$ Å, $b = 17.886(2)$ Å, $c = 10.828(1)$ Å, $\beta = 92.734(2)°$, and $Z = 4$. Compound **7** ($C_{15}H_{13}CuClN_4O_2$) crystallizes in the orthorhombic system, space group $Pna2_1$, with $a = 7.9487(6)$ Å, $b = 14.3336(10)$ Å, $c = 13.0014(9)$ Å, and $Z = 4$. Density functional calculations on PPOCCO are examined in relation to the anti-eclipsed conformational change that occurs on coordination to copper(II).

Introduction

Symmetrical diazine ligands e.g. PAHAP (Chart 1), with two coordination compartments linked by a single N−N bridge, usually produce dinuclear copper(II) complexes, in which the two metal centers are bridged by the N_2 group and also bonded to the peripheral coordination site groupings. This leads to a situation where a variety of different structural types are observed on the basis of the free rotation of the copper coordination planes around the N−N single bond. This in turn leads to a wide variety of magnetic exchange situations, which depend cleanly on the angle of rotation of

* Author to whom correspondence should be addressed. E-mail: lthomp@mun.ca.
[†] Memorial University.
[‡] University of Durham.
[§] University of Nottingham.

10.1021/ic040036i CCC: $27.50
Published on Web 06/11/2004

Chart 1

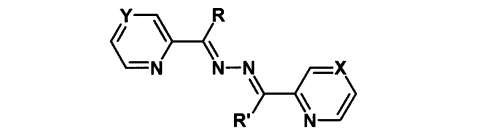

POAP (R=OH, R'=NH_2, X=Y=CH), PAHAP (R=R'=NH_2, X=Y=CH),PZOAPZ (R=OH, R'=NH_2, X=N, Y=N), PMHAP (R=CH_3, R'=NH_2,X=Y=CH), POMP (R=CH_3, R'=OH, X=Y=CH)

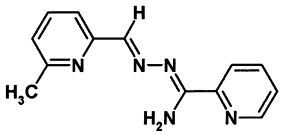

PHMAP

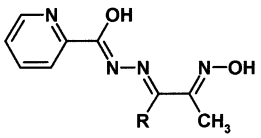

PPOCCO (R=Ph), POCCO (R=CH_3)

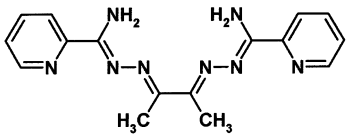

BDPAH

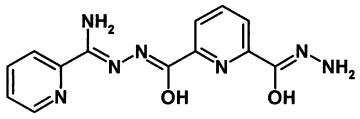

POAHD

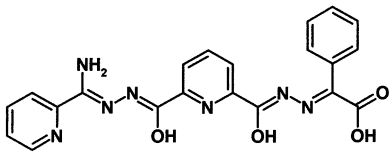

POAPF

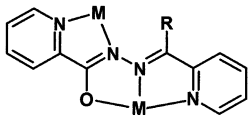

a

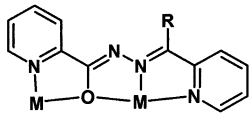

b

the copper magnetic orbitals around the N−N bond. These range from intramolecular ferromagnetism at low angles (<75°) to antiferromagnetism at higher angles, with a linear relationship between exchange integral and rotational angle.[1,2]

The ligand flexibility, combined with the donor rich nature of this type of ligand, leads to a situation where, in addition to rotational variations, different structural motifs occur through various combinations of the diazine and geminal groups and the terminal donor groups. Ligands such as POAP and PZOAPZ (Chart 1) have OH and NH_2 groups adjacent to the diazine, both of which can coordinate, and in many cases polynuclear cluster complexes with four (M(II), M = Mn, Co, Ni, Cu)[3−6,9,10] and five (M(II), M = Mn, Co, Zn)[7−10] metals result, through self-assembly reactions with M(II) salts, in which the metals are bridged by just the alkoxo groups. In other cases, e.g. with PMHAP, PHMAP, and BDPAH (Chart 1), dinuclear structures result, with the complex locked in a close to trans-conformation about the N−N bond by secondary coordination of one NH_2 group (see e.g. $[Cu_2(PMHAP\text{-}H)(NO_3)_3]$ ($-2J$ = 173 cm^{-1}),[1] $[Cu_2(PHMAP\text{-}H)(NO_3)_3(H_2O)(MeOH)]$ ($-2J$ = 208 cm^{-1}),[2] $[Cu_2(BDPAH\text{-}H)(NO_3)_2](NO_3)$ ($-2J$ = 112 cm^{-1})[11]). This leads to large Cu−N−N−Cu torsional angles and quite strong intramolecular antiferromagnetic coupling.[1,2,11]

In this study we report a different type of "locked" structural modification in dinuclear copper(II) bromide complexes of the ligands POAP, PZOAPZ, and PAOPF, in which the alkoxide oxygen atoms are involved in direct coordination to the metal centers, either as a terminal or bridging entity. Structural and magnetic properties for the coordinatively "isomeric" dinuclear complexes $[Cu_2(POAP\text{-}H)Br_3(H_2O)]$ (**1**), $[Cu_2(PZOAPZ\text{-}H)Br_3(H_2O)_2]$ (**2**), and $[Cu_2(PAOPF\text{-}2H)Br_2(DMSO)(H_2O)]$ (**3**) and the tetranuclear complex $[Cu_4(POMP\text{-}H)_4](NO_3)_4\cdot 2H_2O$ (**4**) are reported, in addition to the structures of the mononclear complexes of an oxime extended ligand, PPOCCO (**5**), including [Cu(PPOCCO-H)-(NO_3)] (**6**) and [Cu(PPOCCO-H)Cl] (**7**). Density functional calculations on **2** are presented as a means of better understanding the unusual magnetic behavior of this compound and also on the ligand PPOCCO, which undergoes an anti-eclipsed conformational twist on coordination.

Experimental Section

Physical Measurements. Melting points were measured on a Fisher-Johns melting point apparatus. Infrared spectra were recorded as Nujol mulls using a Mattson Polaris FTIR instrument. Mass

(1) Xu, Z.; Thompson, L. K.; Miller, D. O. *Inorg. Chem.* **1997**, *36*, 3985 and references therein.

(2) Thompson, L. K.; Xu, Z.; Goeta, A. E.; Howard, J. A. K.; Clase, J.; Miller, D. O. *Inorg. Chem.* **1998**, *37*, 3217 and references therein.

(3) Matthews, C. J.; Avery, K.; Xu, Z.; Thompson, L. K.; Zhao, L.; Miller, D. O.; Biradha, K.; Poirier, K.; Zaworotko, M. J.; Wilson, C.; Goeta, A. E.; Howard, J. A. K. *Inorg. Chem*. **1999**, *38*, 5266.

(4) Thompson, L. K.; Matthews, C. J.; Zhao, L.; Xu, Z.; Miller, D. O.; Wilson, C.; Leech, M. A.; Howard, J. A. K.; Heath, S. L.; Whittaker, A. G.; Winpenny, R. E. P. *J. Solid State Chem*. **2001**, *159*, 308.

(5) Xu, Z.; Thompson, L. K.; Matthews, C. J.; Miller, D. O.; Goeta, A. E.; Howard, J. A. K. *Inorg. Chem*. **2001**, *40*, 2446.

(6) Xu, Z.; Thomspon, L. K.; Miller, D. O. *J. Chem. Soc., Dalton Trans*. **2002**, 2462.

(7) Matthews, C. J.; Xu, Z.; Mandal, S. K.; Thompson, L. K.; Biradha, K.; Poirier, K.; Zaworotko, M. J. *J. Chem. Soc., Chem. Commun*. **1999**, 347.

(8) Matthews, C. J.; Thompson, L. K.; Parsons, S. R.; Xu, Z.; Miller, D. O.; Heath, S. L. *Inorg. Chem*. **2001**, *40*, 4448.

(9) Zhao, L.; Matthews, C. J.; Xu, Z.; Thompson, L. K.; Miller, D. O. Mol. *Cryst. Liq. Cryst*. **2002**, *376*, 389.

(10) Thompson, L. K. *Coord. Chem. Rev*. **2002**, *233−234*, 193.

(11) Xu, Z.; Thompson, L. K.; Matthews, C. J.; Miller, D. O.; Goeta, A. E.; Wilson, C.; Howard, J. A. K.; Ohba, M.; Ôkawa, H. *J. Chem. Soc., Dalton Trans*. **2000**, 69.

spectra were obtained with VG Micromass 7070HS (EI) and HP1100MSD (LCMS) spectrometers. C, H, and N analyses on vacuum-dried samples were performed by the Canadian Microanalytical Service, Delta, BC, Canada. Variable-temperature magnetic data were obtained with a Quantum Design MPMS5S Squid magnetometer operating in the range 0.1−1.0 T (2−300 K). Calibrations were carried out with a palladium standard sample, and temperature errors were checked with $[H_2TMEN][CuCl_4]$ ($H_2TMEN = (CH_3)_2HNCH_2CH_2NH(CH_3)_2^{2+}$).[12]

Materials. Commercially available solvents and chemicals were used, without further purification.

Ligand Preparations. PAOPF. The half-hydrazide POAHD[13] (Chart 1) (1.01 g, 0.0034 mol) was suspended in methanol (50 mL). Benzoylformic acid (0.51 g, 0.0034 mol) dissolved in a few milliliters of methanol was added, and the suspension refluxed overnight. The solid became noticeably whiter as the reaction proceeded. Filtration gave 1.04 g (yield 71%) of crude PAOPF. The product was recrystallized by dissolving in hot DMSO and adding acetone. Anal. Calcd for $C_{21}H_{17}N_7O_4$: C, 58.47; H, 3.94; N, 22.74. Found: C, 58.12; H, 3.90; N, 22.20.

POMP. 2-Acetylpyridine (1.8 g, 15.0 mmol) was added dropwise to a solution of picolinic hydrazide (1.35 g, 10.0 mmol) in 15 mL of methanol. The resulting solution was refluxed for 6 h. A noticeable cloudiness of the solution was observed within 1 h. A white precipitate was formed, which was filtered off, washed with methanol and ether, and vacuum-dried (yield 83%). Mp: 195−197 °C. Mass spectrum (*m*/*z*): 241 (MH^+), 134, 106, 78. IR (ν, cm^{-1}): 3316 (NH), 1701 (CO), 995 (py). NMR (DMSO-d_6, ppm): 2.5 (s, CH_3), 7.45 (t), 7.72 (t), 7.90 (t), 8.11 (t), 8.16 (t), 8.64 (d), 8.75 (d), 11.15 (s, OH). Anal. Calcd for $C_{13}H_{12}N_4O$: C, 64.98; H, 5.03; N, 23.31. Found: C, 64.69; H, 5.10; N, 23.07.

PPOCCO (5). 1-Phenyl-1,2-propanedione-2-oxime (1.69 g, 0.0103 mol) was dissolved in 20 mL of absolute ethanol. Picolinic acid hydrazide (1.42 g, 0.0103 mol) was added. Refluxing overnight produced a pale yellow colored solution, which gave a white precipitate on cooling. The precipitate was washed with ethanol and vacuum-dried. Further evaporation of the solution gave more product (yield 1.76 g; 60%). Mp: 218.5−219.5 °C. Mass spectrum (major mass peaks, *m*/*z*): 265 (M − H_2O), 224 (M − oxime group), 176 (M − O═C−pyr), 106 (O═C−pyr), 78, (py), 77 (Ph). IR (ν, cm^{-1}): 3234 (N−H, vs, br), 1680 (s, C═O), 1507 (vs, C═N), 1014 (N−O). Anal. Calcd for $C_{15}H_{14}N_4O_2$: C, 63.83; H, 4.96; N, 19.86. Found: C, 63.85; H, 5.15; N, 19.74.

Complex Preparations. $[Cu_2(POAP\text{-}H)Br_3(H_2O)]$ (1). POAP (0.241 g, 1.00 mmol) was suspended in a solution of copper(II) bromide (0.67 g, 3.0 mmol) in 20 mL of deionized water at room temperature. A 10 mL volume of ethanol was added forming a dark green solution, which was filtered and allowed to stand at room temperature for several days. Black crystals formed, suitable for a structural analysis (yield 0.50 g, 71%). The structure revealed an extra water molecule in the crystalline sample (vide infra). Anal. Calcd for $Cu_2(C_{12}H_{10}N_5O)(H_2O)Br_3$: C, 23.06; H, 1.94; N, 11.20. Found: C, 23.69; H, 1.74; N, 11.42.

$[Cu_2(PZOAPZ\text{-}H)Br_3(H_2O)_2]$ (2). PZOAPZ (0.243 g, 1.00 mmol) was added to a solution of $CuBr_2$ in a mixture of water (15 mL) and methanol (10 mL), and the mixture was warmed. A dark green solution formed which deposited dark green crystals on cooling, which were suitable for a structural determination. (yield 0.14 g, 22%). Anal. Calcd for $(C_{10}H_9N_7O)Cu_2Br_3(H_2O)_2$: C, 18.72; H, 1.87; N, 15.29. Found: C, 19.16; H, 1.68; N, 15.51.

$[Cu_2(PAOPF\text{-}2H)Br_2(DMSO)(H_2O)]$ (3). A solution of PAOPF (0.0703 g, 0.160 mmol) in 2 mL of DMSO was added to a DMSO solution (2 mL) of $CuBr_2$ (0.0797 g, 0.35 mmol), giving a dark green-brown colored solution. Slow diffusion of acetone into the solution gave moss-green platelike crystals, plus a light green powder. The crystals were suitable for a structural determination. However, it proved very difficult to produce a homogeneous sample of this compound, and magnetic data (vide infra) suggest that it is a mixture.

$[Cu_4(POMP\text{-}H))_4](NO_3)_4\cdot 2H_2O$ (4). A 0.10 g (0.40 mmol) amount of POMP was added to a solution of 0.20 g (0.80 mmol) of $Cu(NO_3)_2\cdot 3H_2O$ dissolved in a methanol/H_2O (20 mL/5 mL) mixture with stirring. The ligand dissolved forming a deep clear blue solution. A few drops of Et_3N were added, and stirring was continued overnight. The solution was filtered and kept for crystallization. Dark blue crystals suitable for X-ray analysis were obtained after 2 weeks (yield 66%). Anal. Calcd for $[(C_{13}H_{11}N_4O)_4Cu_4](NO_3)_4\cdot 2H_2O$: C, 41.76; H, 3.23; N, 18.73. Found: C, 41.41; H, 3.28; N, 18.31.

$[Cu(PPOCCO\text{-}H)(NO_3)]$ (6). PPOCCO (0.045 g, 0.16 mmol) was dissolved in 20 mL of ethanol. A solution of $Cu(NO_3)_2\cdot 3H_2O$ (0.039 g, 0.16 mmol) in ethanol (3 mL) was added slowly. The solution turned immediately yellow-brown and was stirred at about 60 °C for $^1/_2$ hour and filtered. On cooling and slow evaporation small thin brown needles suitable for X-ray structural determination were obtained (yield 35%). Anal. Calcd for $(C_{15}H_{13}N_4O_2)$-$Cu(NO_3)$: C, 44.22; H, 3.47; N, 17.20. Found: C, 44.33; H, 3.35; N, 17.08.

$[Cu(PPOCCO\text{-}H)Cl]$ (7). A solution of $CuCl_2\cdot 2H_2O$ (0.036 g, 0.21 mmol) in 5 mL of ethanol was added to a warm (60 °C) solution of PPOCCO (0.062 g, 0.22 mmol) in 5 mL of ethanol, forming a dark green solution. Cooling and evaporation at room temperature gave green needles suitable for X-ray structural determination (yield 30%). Anal. Calcd for $(C_{15}H_{13}N_4O_2)CuCl$: C, 47.37; H, 3.71; N, 14.74. Found: C, 47.35; H, 3.49; N, 14.85.

Crystallography. Diffraction data for single crystals of **1** and **2** (**1**, dark green, almost black, 0.30 × 0.14 × 0.08 mm; **2**, dark green fragment cut from block 0.30 × 0.30 × 0.30 mm) were collected using a Bruker SMART CCD diffractometer, equipped with an Oxford Cryostream N_2 cooling device,[14] with graphite-monochromatized Mo Kα radiation. Cell parameters were determined and refined using the SMART software,[15a] raw frame data were integrated using the SAINT program,[15b] and the structures were solved using direct methods and refined by full-matrix least squares on F^2 using SHELXTL.[16] Non-hydrogen atoms were refined with anisotropic atomic displacement parameters (adps). Hydrogen atoms bound to carbon atoms were placed in geometrically calculated positions with isotropic adps 1.2 times that of the parent atom.

The diffraction intensities of single crystals of **3** and **5** (**3**, brown-green plate, dimensions 0.42 × 0.18 × 0.05 mm; **5**, colorless, irregular crystal 0.41 × 0.19 × 0.38 mm) were collected with graphite-monochromated Mo Kα X-radiation using a Rigaku AFC6S diffractometer at 299(1) K and the $\omega-2\theta$ scan technique to a 2θ value of 55.1°. The data were corrected for Lorentz and

(12) Brown, D. S.; Crawford, V. H.; Hall, J. W.; Hatfield, W. E. *J. Phys. Chem.* **1977**, *81*, 1303.
(13) Milway, V. A.; Zhao, L.; Abedin, T. S. M.; Thompson, L. K.; Xu, Z. *Polyhedron* **2003**, *22*, 1271.
(14) Cosier, J.; Glazer, A. M. *J. Appl. Crystallogr.* **1986**, *19*, 105.
(15) (a) *Siemens SMART Data Collection Software*, ver. 4.050; Siemens Analytical X-ray Instruments Inc.: Madison, WI, 1996. (b) *Siemens SAINT Data Reduction Software*, version 4.050; Siemens Analytical X-ray Instruments Inc.: Madison, WI, 1996.
(16) Sheldrick, G. M. *SHELXTL 5.04/VMS, An integrated system for solving, refining and Displaying crystal structures from diffraction data*; Siemens Analytical X-ray Instruments Inc.: Madison, WI, 1995.

Table 1. Summary of Crystallographic Data for **1**−**7**

param	**1**	**2**	**3**	**4**	**5**	**6**	**7**
empirical formula	$C_{12}H_{16}Br_3N_5Cu_2O_4$	$C_{10}H_{13}Br_3Cu_2N_7O_4$	$C_{23}H_{22}Cu_2Br_2N_7O_{5.5}S$	$C_{52}H_{48}Cu_4N_{20}O_{18}$	$C_{15}H_{14}N_4O_2$	$C_{15}H_{13}CuN_5O_5$	$C_{15}H_{13}CuClN_4O_2$
M_r	661.11	662.08	803.43	1495.26	282.30	406.84	380.29
cryst syst	monoclinic	triclinic	monoclinic	monoclinic	orthorhombic	monoclinic	orthorhombic
space group	$P2_1/c$	$P\bar{1}$	$P2_1/c$ (No. 14)	$P2_1/n$	$Pna2_1$	$P2_1/c$	$Pna2_1$
a/Å	15.1465(3)	9.1413(1)	12.406(2)	14.4439(6)	7.834(3)	8.2818(9)	7.9487(6)
b/Å	18.1848(12)	10.4723(1)	22.157(3)	12.8079(5)	11.797(4)	17.886(2)	14.3336(10)
c/Å	6.8557(5)	10.9411(1)	10.704(2)	16.4240(7)	15.281(3)	10.8284(12)	13.0014(9)
α/deg	90	100.769(1)	90	90	90	90	90
β/deg	92.751(4)	106.271(1)	106.21(1)	105.199(1)	90	92.734(2)	90
γ/deg	90	103.447(1)	90	90	90	90	90
V/Å^3	1886.13(19)	941.58(2)	2825.2(8)	2932.1(2)	1412.1(6)	1602.2(3)	1481.29(18)
ρ_{calcd}/g cm^{-3}	2.328	2.335	1.889	1.694	1.328	1.687	1.705
T/K	150(2)	293(2)	299(1)	193(2)	293(2)	193(2)	193(2)
Z	4	2	4	2	4	4	4
μ/cm^{-1}	8.639	8.656	44.67	1.523	0.92	13.79	16.69
reflns collcd							
tot., unique, R_{int}	17 461, 3710, 0.0473	10 796, 4288, 0.0299	7035, 6692, 0.080	20 796, 5986, 0.0356	1902, 838, 0.0299	1472, 3282, 0.046	10 966, 3018, 0.021
obsd ($I > 2.00\sigma(I)$)	3093	3623	3006	4768	838	2561	3018
final R_1, wR_2[a]	0.0419, 0.0980	0.0279, 0.0529	0.065 (R), 0.059 (R_w)	0.0359, 0.0856	0.05 (R), 0.044 (R_w)	0.0492, 0.1235	0.0221, 0.0594

[a] $R_1 = \sum[|F_o| - |F_c|]/\sum|F_o|$; $wR_2 = [\sum[w(|F_o|^2 - |F_c|^2)^2]/\sum[w(|F_o|^2)^2]]^{1/2}$. $R = \sum||F_o| - |F_c||/\sum|F_o|$; $R_w = [\sum w(|F_o| - |F_c|)^2/\sum wF_o^2]^{1/2}$.

polarization effects, and the structures solved by direct methods.[17,18] All atoms except hydrogen were refined anisotropically. Hydrogen atoms were introduced with isotropic thermal parameters set 20% greater than those of their bonded partners at the time of their inclusion. They were optimized by positional refinement. Neutral atom scattering factors[19] and anomalous-dispersion terms[20,21] were taken from the usual sources. All calculations were performed with the teXsan[22] crystallographic software package using a PC computer.

The diffraction intensities of single crystals of **4**, **6**, and **7** (**4**, green plate, dimensions 0.45 × 0.17 × 0.08 mm; **6**, dark green rod; dimensions 0.57 × 0.12 × 0.0 mm; **7**, red-brown prism, 0.63 × 0.29 × 0.14 mm) were collected with graphite-monochromatized Mo Kα X-radiation (rotating anode generator) using a Bruker P4/CCD diffractometer at 193(2) K to a maximum 2θ value of 52.8°. The data were corrected for Lorentz and polarization effects. The structure was solved by direct methods.[17,18] All atoms except hydrogens were refined anisotropically. Hydrogen atoms were placed in calculated positions with isotropic thermal parameters set to 20% greater than their bonded partners and were not refined. Neutral atom scattering factors[19] and anomalous-dispersion terms[20,21] were taken from the usual sources. All other calculations were performed with the teXsan[22] crystallographic software package using a PC computer.

Abbreviated structural data for **1**−**7** are reported in Table 1 and have reference CCDC Nos. 232797−232803 for **1**−**7**. See http://www.rsc.org/suppdata/dt/bl/****** for crystallographic data in CIF format.

Computational Details

Recent work in the area of density functional theory has shown the utility of the hybrid functional[23] B3LYP in calculating accurate estimates of the exchange coupling constant for transition-metal complexes.[24−26] The triplet energy is calculated directly, whereas a modified broken-symmetry approach[27] is utilized to obtain the energy of the singlet state. The B3LYP functional and 6-311G(d) basis set were used as implemented by Gaussian03.[28] Conformational studies on the ligand PPOCCO **(5)** (including optimized geometries and calculation of vibrational frequencies) were carried out at the B3LYP/6-31G(d) level of theory.

Results and Discussion

Structures. [Cu_2(POAP-H)Br_3(H_2O)] (1). A structural representation for the dinuclear complex **1** is shown in Figure

(17) (a) Sheldrick, G. M. *SHELX97*; University of Gottingen: Gottingen, Germany, 1997. (b) SIR97: Altomare, A.; Cascarano, M.; Giacovazzo, C.; Guagliardi, A. *J. Appl. Crystallogr.* **1993**, *26*, 343.

(18) DIRDIF94: Beurskens, P. T.; Admiraal, G.; Beurskens, G.; Bosman, W. P.; de Gelder, R.; Israel, R.; Smits, J. M. M. *The DIRDIF-94 program system*; Technical Report of the Crystallography Laboratory; University of Nijmegen: Nijmegen, The Netherlands, 1994.

(19) Cromer, D. T.; Waber, J. T. *International Tables for X-ray Crystallography*; The Kynoch Press: Birmingham, England, 1974; Vol. IV, Table 2.2 A.

(20) Ibers, J. A.; Hamilton, W. C. *Acta Crystallogr.* **1964**, *17*, 781.

(21) Creagh, D. C.; McAuley, W. J. *International Tables for Crystallography*; Wilson, A. J. C., Ed.; Kluwer Academic Publishers: Boston, MA, 1992; Vol. C, Table 4.2.6.8, pp 219−222.

(22) *teXsan for Windows*: *Crystal Structure Analysis Package*; Molecular Structure Corp: The Woodlands, TX, 1997.

(23) Becke, A. D. *J. Chem. Phys.* **1993**, *98*, 5648.

(24) Xu, Z.; Thompson, L. K.; Miller, D. O.; Ruiz, E.; Alvarez, S. *Inorg. Chem.* **2003**, *42*, 1107.

(25) Chen, Z.; Xu, Z.; Zhang, L.; Yan, F.; Lin, Z. *J. Phys. Chem. A* **2001**, *105*, 9710.

(26) Ruiz, E.; Alemany, P.; Alvarez, S.; Cano, J. *J. Am. Chem. Soc.* **1997**, *119*, 1297.

(27) Ruiz, E.; Cano, J.; Alvarez, S.; Alemany, P. *J. Comput. Chem.* **1999**, *20*, 1391.

(28) Frisch, M. J.; Trucks, G. W.; Schlegel, H. B.; Scuseria, G. E.; Robb, M. A.; Cheeseman, J. R.; Montgomery, J. A., Jr.; Vreven, T.; Kudin, K. N.; Burant, J. C.; Millam, J. M.; Iyengar, S. S.; Tomasi, J.; Barone, V.; Mennucci, B.; Cossi, M.; Scalmani, G.; Rega, N.; Petersson, G. A.; Nakatsuji, H.; Hada, M.; Ehara, M.; Toyota, K.; Fukuda, R.; Hasegawa, J.; Ishida, M.; Nakajima, T.; Honda, Y.; Kitao, O.; Nakai, H.; Klene, M.; Li, X.; Knox, J. E.; Hratchian, H. P.; Cross, J. B.; Adamo, C.; Jaramillo, J.; Gomperts, R.; Stratmann, R. E.; Yazyev, O.; Austin, A. J.; Cammi, R.; Pomelli, C.; Ochterski, J. W.; Ayala, P. Y.; Morokuma, K.; Voth, G. A.; Salvador, P.; Dannenberg, J. J.; Zakrzewski, V. G.; Dapprich, S.; Daniels, A. D.; Strain, M. C.; Farkas, O.; Malick, D. K.; Rabuck, A. D.; Raghavachari, K.; Foresman, J. B.; Ortiz, J. V.; Cui, Q.; Baboul, A. G.; Clifford, S.; Cioslowski, J.; Stefanov, B. B.; Liu, G.; Liashenko, A.; Piskorz, P.; Komaromi, I.; Martin, R. L.; Fox, D. J.; Keith, T.; Al-Laham, M. A.; Peng, C. Y.; Nanayakkara, A.; Challacombe, M.; Gill, P. M. W.; Johnson, B.; Chen, W.; Wong, M. W.; Gonzalez, C.; Pople, J. A. *Gaussian 03*, revision B.05; Gaussian, Inc.: Pittsburgh, PA, 2003.

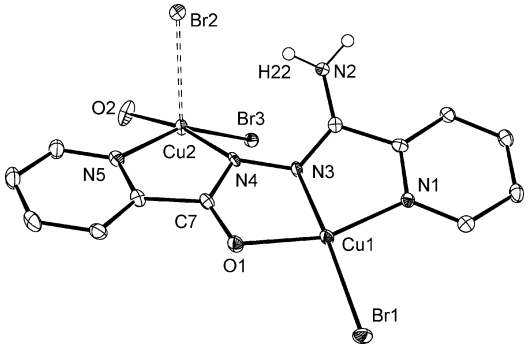

Figure 1. Structural representation for **1** (40% probability thermal ellipsoids).

Table 2. Distances (Å) and Angles (deg) for $[Cu_2(POAP\text{-}H)Br_3(H_2O)]$ (**1**)

Br1−Cu1	2.3210(10)	Cu1−N1	1.996(5)
Br2−Cu2	2.7213(11)	Cu2−O2	1.988(5)
Br3−Cu2	2.3969(10)	Cu2−N4	2.000(5)
Cu1−N3	1.914(5)	Cu2−N5	2.028(6)
Cu1−O1	1.979(5)		
N3−Cu1−O1	81.0(2)	N4−Cu2−N5	80.0(2)
N3−Cu1−N1	81.2(2)	O2−Cu2−Br3	87.34(16)
O1−Cu1−N1	160.2(2)	N4−Cu2−Br3	93.88(15)
N3−Cu1−Br1	167.57(17)	N5−Cu2−Br3	152.22(16)
O1−Cu1−Br1	99.58(13)	O2−Cu2−Br2	94.28(17)
N1−Cu1−Br1	99.63(16)	N4−Cu2−Br2	95.89(15)
O2−Cu2−N4	168.4(2)	N5−Cu2−Br2	95.26(16)
O2−Cu2−N5	93.6(2)	Br3−Cu2−Br2	112.38(4)

1, and important bond distances and angles are listed in Table 2. Two square pyramidal copper(II) centers are bridged by the N−N diazine fragment of the tetradentate ligand, with a Cu1−Cu2 separation of 4.718 Å and a Cu−N−N−Cu torsional angle of 150.5°. Equatorial terminal bromine atoms are bound to Cu2 and Cu1 (Cu−Br 2.397 and 2.321 Å, respectively), with another associated axially with Cu2, with a very long Cu−Br separation (2.721 Å). A water molecule (O2) completes the basal coordination sphere for Cu2. This water molecule is hydrogen bonded to a second lattice water molecule (O2−O3 2.661 Å). The charge balance requires that the ligand is deprotonated. Establishing the site of deprotonation of ligands in this class is sometimes difficult because of charge delocalization within the ligand backbone. However a short Cu1−O1 distance (1.979(5) Å) and relatively long C7−O1 distance (1.275 Å) suggest that O1 is the principal site of deprotonation. The coordination of O1 as a terminal donor to Cu1 has the effect of fixing the conformation of the complex as it pertains to the Cu−N−N−Cu torsional angle. The NH_2 group (N2) points toward the axial bromine Br2 (Br2−N2 3.459 Å), with a possible weak hydrogen-bonding interaction, but it seems unlikely that this contact influences the overall complex conformation.

$[Cu_2(PZOAPZ\text{-}H)Br_3(H_2O)_2]$ (2). The structure of the dinuclear complex **2** is shown in Figure 2, and important bond distances and angles are listed in Table 3. The two square-pyramidal copper(II) centers are bridged differently in this case by a single alkoxide oxygen atom, with the ligand PZOAPZ again acting in a tetradentate fashion. The Cu−O distances to the oxygen bridge are quite different (Cu1−O1

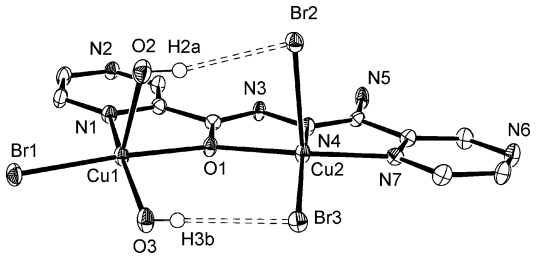

Figure 2. Structural representation for **2** (40% probability thermal ellipsoids).

Table 3. Distances (Å) and Angles (deg) for $[Cu_2(PZOAPZ\text{-}H)Br_3(H_2O)_2]$ (**2**)

Br1−Cu1	2.3832(5)	Cu1−O2	2.273(3)
Br2−Cu2	2.6518(6)	Cu2−N4	1.916(3)
Br3−Cu2	2.3956(5)	Cu2−N7	2.065(3)
Cu1−O3	1.967(3)	Cu2−O1	2.157(2)
Cu1−N1	2.009(3)	N3−N4	1.389(4)
Cu1−O1	2.047(2)		
O3−Cu1−N1	162.20(12)	N4−Cu2−O1	76.95(10)
O3−Cu1−O1	89.33(11)	N7−Cu2−O1	155.20(10)
N1−Cu1−O1	82.50(10)	N4−Cu2−Br3	162.49(9)
O3−Cu1−O2	94.70(12)	N7−Cu2−Br3	98.11(8)
N1−Cu1−O2	100.01(12)	O1−Cu2−Br3	102.99(6)
O1−Cu1−O2	83.48(10)	N4−Cu2−Br2	99.30(9)
O3−Cu1−Br1	89.73(9)	N7−Cu2−Br2	99.52(8)
N1−Cu1−Br1	97.17(8)	O1−Cu2−Br2	90.28(7)
O1−Cu1−Br1	175.46(7)	Br3−Cu2−Br2	98.21(2)
O2−Cu1−Br1	101.02(8)	Cu1−O1−Cu2	141.70(12)
N4−Cu2−N7	79.01(11)		

2.047(2) Å, Cu2−O1 2.157(2) Å), with a very large Cu−O−Cu angle (141.7(1)°), leading to a substantially shorter Cu−Cu separation (3.973 Å) than observed for **1**. Bromine atoms are bound equatorially to each copper center (Cu1−Br1 2.3832(5) Å, Cu2−Br3 2.3956(5) Å), with a long axial bromine contact to Cu2 (2.6518(6) Å). Cu1 has two coordinated water molecules, one in the equatorial plane (Cu1−O3 1.967(3) Å) and the other in a axial position (Cu1−O2 2.273(3) Å). The overall molecule is almost flat, with the copper basal planes coinciding with the ligand "plane". The copper atoms are displaced slightly from the basal toward the apical ligands.

The essentially flat arrangement of the copper basal planes and the ligand can be attributed in part to the contiguous "linear" grouping of three five-membered chelate rings. However the close proximity of the hydrogen atoms on coordinated water molecules O2 and O3 and Br2 and Br3, respectively (H2a−Br2 2.503 Å, H3b−Br3 2.568 Å), indicates that significant hydrogen-bonding contacts also contribute to the structural arrangement (Figure 2). An extended weak interaction associates individual molecules into pairs (Figure 3), with long pseudoaxial Cu1−Br3 and Cu2−O3 contacts (3.422, 3.045 Å, respectively). These are considered to be too weak to have any significant influence on e.g. the magnetic properties.

$[Cu_2(PAOPF\text{-}2H)Br_2(DMSO)(H_2O)]\cdot H_2O$ (3). The structure of the dinuclear complex **3** is shown in Figure 4, and important bond distances and angles are listed in Table 4. Two square pyramidal copper(II) centers are bridged at a distance of 4.890 Å by the diazine N−N group from the pyridine amidrazone end of the asymmetric ligand, with an

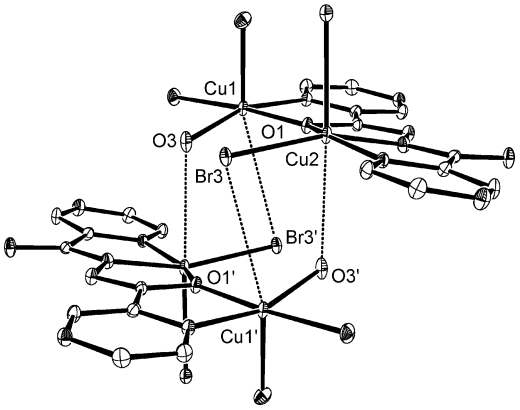

Figure 3. Structural representation of the associated structure in **2**.

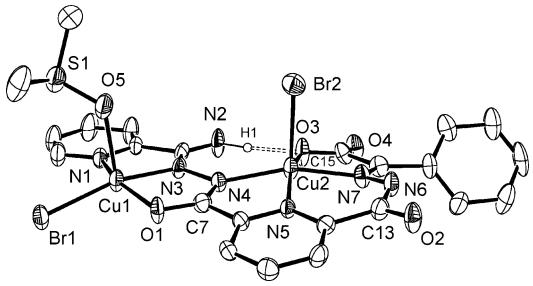

Figure 4. Structural representation for **3** (30% probability thermal ellipsoids).

Table 4. Distances (Å) and Angles (deg) for $[Cu_2(PAOPF\text{-}2H)Br_2(DMSO)(H_2O)]$ (**3**)

Br1−Cu1	2.382(2)	Cu1−N3	1.944(8)
Br2−Cu2	2.579(2)	Cu2−O3	1.937(7)
Cu1−O1	1.977(7)	Cu2−N4	2.055(8)
Cu1−O5	2.261(8)	Cu2−N5	1.973(8)
Cu1−N1	2.013(9)	Cu2−N7	2.007(8)
Br1−Cu1−O1	97.7(2)	Br2−Cu2−O3	103.0(3)
Br1−Cu1−O5	98.7(2)	Br2−Cu2−N4	101.9(2)
Br1−Cu1−N1	98.9(2)	Br2−Cu2−N5	95.9(2)
Br1−Cu1−N3	164.3(3)	Br2−Cu2−N7	94.8(3)
O1−Cu1−O5	99.2(3)	O3−Cu2−N4	101.4(3)
O1−Cu1−N1	157.9(3)	O3−Cu2−N5	159.2(4)
O1−Cu1−N3	79.9(3)	O3−Cu2−N7	79.8(3)
O5−Cu1−N1	92.5(3)	N4−Cu2−N5	82.8(3)
O5−Cu1−N3	97.0(3)	N4−Cu2−N7	162.4(4)
N1−Cu1−N3	80.2(3)	N5−Cu2−N7	90.2(3)

almost trans arrangement of the copper basal planes relative to the N−N bond (Cu1−N2−N3−Cu2 torsional angle 162°). Cu2 is coordinated by a basal arrangement of two diazine nitrogens, a pyridine nitrogen atom, and a carboxylate oxygen (Cu−L 1.93−2.06 Å). Cu1 binds to a diazine and a pyridine nitrogen, an alkoxide oxygen, and a terminal bromine in the basal plane (Cu−L 1.94−2.39 Å). A DMSO molecule coordinates axially to Cu1, and a bromine coordinates axially to Cu2 (Cu1−O5 2.261(8) Å; Cu2−Br2 2.579(2) Å). The short Cu1−O1 distance (1.977(7) Å) and the relatively long C7−O1 distance (1.27(1) Å) indicates a deprotonated, alkoxide type oxygen center. Since the formula indicates the loss of two protons from the ligand, a proton must remain on the other half of the ligand bonded to Cu2. The very short Cu2−O3 contact (1.937(7) Å) clearly indicates that the carboxylic subunit is negatively charged, and the short C13−O2 distance (1.20(1) Å) suggests that

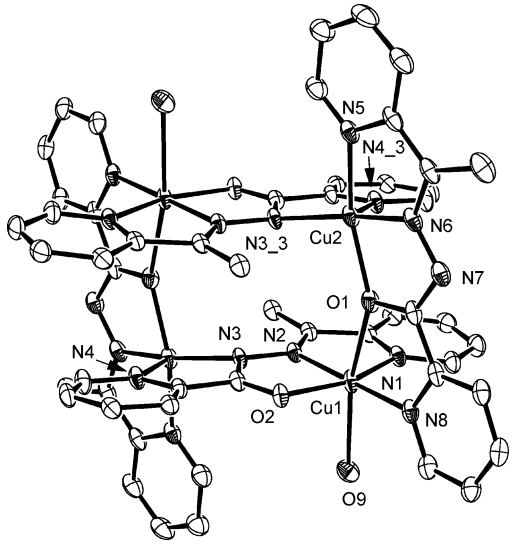

Figure 5. Structural representation for **4** (40% probability thermal ellipsoids).

Table 5. Distances (Å) and Angles (deg) for $[Cu_4(POMP\text{-}H)_4](NO_3)_4\cdot 2H_2O$ (**4**)

Cu1−N2	1.943(2)	Cu2−O1	2.017(2)
Cu1−N8	1.994(2)	Cu2−N5	2.019(2)
Cu1−O2	1.9971(18)	Cu2−N3	2.026(2)
Cu1−N1	2.009(2)	Cu2−N4	2.172(2)
Cu1−O1	2.3305(18)	N2−N3	1.386(3)
Cu2−N6	1.923(2)	N4−Cu2	2.172(2)
N2−Cu1−N8	178.16(9)	N6−Cu2−N5	80.19(10)
N2−Cu1−O2	79.99(8)	O1−Cu2−N5	158.34(9)
N8−Cu1−O2	98.73(8)	N6−Cu2−N3	163.94(9)
N2−Cu1−N1	79.91(9)	O1−Cu2−N3	99.34(8)
N8−Cu1−N1	101.33(9)	N5−Cu2−N3	99.78(9)
O2−Cu1−N1	159.88(9)	N6−Cu2−N4	117.36(9)
N2−Cu1−O1	101.66(8)	O1−Cu2−N4	94.24(9)
N8−Cu1−O1	76.94(8)	N5−Cu2−N4	99.42(9)
O2−Cu1−O1	88.41(7)	N3−Cu2−N4	78.59(8)
N1−Cu1−O1	94.65(8)	Cu2−O1−Cu1	141.23(9)
N6−Cu2−O1	78.62(9)		

the site of protonation is probably the uncoordinated diazine N6. Additional support comes from the distances within the N7−N6−C13 fragment (1.36(1) and 1.35(1) Å), which suggest an sp^3 type nitrogen center.

The almost trans orientation of the copper basal planes relative to the N−N diazine bridge is fixed mainly by the Cu1−O1 bond. However, a short hydrogen-bonded N2−O3 contact (2.671(9) Å; O3−H22−N2 176°) adds an extra, but minor component, which contributes to the molecular conformation.

$[Cu_4(POMP\text{-}H)_4](NO_3)_4\cdot 2H_2O$ (4). The structure of the tetranuclear complex **4** is shown in Figure 5, and important bond distances and angles are listed in Table 5. The ligand POMP self-assembles in the presence of copper nitrate to give a rectangular [2 × 2] grid complex, with two ligands bridging adjacent Cu(II) ions on the short sides of the rectangle with an alkoxide oxygen and two bridging the adjacent Cu(II) ions on the long sides of the rectangle with N−N diazine groups. The Cu1 ions are six coordinate with a water molecule forming the sixth bond (Cu1−O9 2.486 Å). The Cu2 ions are five-coordinate, square-pyramidal, with access to the sixth copper axial coordination site blocked

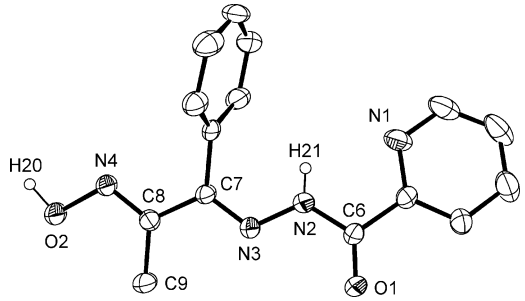

Figure 6. Structural representation for **5** (50% probability thermal ellipsoids).

Table 6. Distances (Å) and Angles (deg) for PPOCCO (**5**)

O1−C6	1.218(7)	C4−C5	1.383(9)
O2−N4	1.400(6)	C5−C6	1.495(8)
N1−C1	1.319(9)	C7−C8	1.467(8)
N1−C5	1.342(7)	C7−C10	1.516(8)
N2−N3	1.368(7)	C8−C9	1.492(8)
N2−C6	1.354(7)	C10−C11	1.379(9)
N3−C7	1.280(7)	C10−C15	1.394(9)
N4−C8	1.283(7)	C11−C12	1.375(9)
C1−C2	1.39(1)	C12−C13	1.38(1)
C2−C3	1.34(1)	C13−C14	1.38(1)
C3−C4	1.37(1)	C14−C15	1.381(9)
C1−N1−C5	117.2(7)	N3−C7−C8	117.2(5)
N3−N2−C6	121.9(5)	N3−C7−C10	122.3(5)
N2−N3−C7	116.6(5)	C8−C7−C10	120.5(5)
O2−N4−C8	111.3(5)	N4−C8−C7	115.4(5)
N1−C1−C2	123.0(7)	N4−C8−C9	124.7(6)
C1−C2−C3	119.3(7)	C7−C8−C9	119.9(5)
C2−C3−C4	119.1(8)	C7−C10−C11	119.2(6)
C3−C4−C5	118.7(7)	C7−C10−C15	120.3(6)
N1−C5−C4	122.7(6)	C11−C10−C15	120.0(6)
N1−C5−C6	116.4(6)	C10−C11−C12	119.6(7)
C4−C5−C6	120.8(6)	C11−C12−C13	121.0(7)
O1−C6−N2	124.8(6)	C12−C13−C14	119.3(6)
O1−C6−C5	123.7(6)	C13−C14−C15	120.7(7)
N2−C6−C5	111.5(5)	C10−C15−C14	119.3(7)

by the presence of the methyl group on the N−N bridging ligands (C27−Cu2 3.203 Å). Cu−Cu separations are 4.813 Å (long) and 4.102 Å (short), with a Cu−O−Cu angle of 141.2° and a Cu−N−N−Cu torsional angle of 159.2°. The basal plane of the square-pyramid at Cu2 includes O1, N3, N5, and N6, with the long axial contact to N4 (Cu2−N4 2.172 Å). For Cu1 the Jahn−Teller axis is defined as O9−Cu1−O1 (Cu1−O9 2.486 Å, Cu1−O1 2.331 Å), with the equatorial plane including O2, N1, N2, and N8. The copper magnetic orbitals coincide with the equatorial planes, and so connections via the alkoxide bridges are strictly orthogonal, while those via the N−N bridge are nonorthognal (vide infra).

Ligand PPOCCO (5). A structural representation for the ligand PPOCCO (**5**) is shown in Figure 6, and important bond distances and angles are listed in Table 6. The ligand backbone, including the pyridine ring, is fairly flat, with protons residing on N2 and O2. The CO bond (C6−O1 1.218 Å) is a double bond. The phenyl ring is twisted relative to the general ligand plane by about 70°, and the methyl group and phenyl ring are arranged in an anti conformation (C9−C8−C7−C10 torsional angle 179.7°). The extended structure shows hydrogen-bonding connectivity between H20 and O1 (O1−O2 2.764 Å; O1−H20−O2 162°), which leads to an intricate interdigitated arrangement (Figure 7), in which the

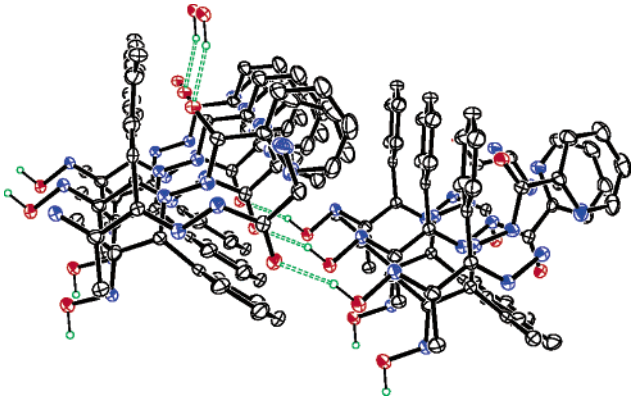

Figure 7. Extended structure of **5** showing hydrogen bonds and interdigitation.

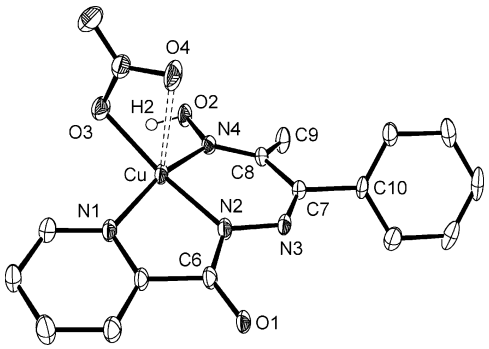

Figure 8. Structural representation for **6** (35% probability thermal ellipsoids).

Table 7. Distances (Å) and Angles (deg) for [Cu(PPOCCO-H)(NO_3)] (**6**)

Cu−N2	1.926(3)	Cu−O3	1.988(3)
Cu−N4	1.947(3)	Cu−O4	2.530(3)
Cu−N1	1.966(3)		
N2−Cu−N4	90.18(12)	N2−Cu−O3	160.07(13)
N2−Cu−N1	83.32(12)	N4−Cu−O3	100.04(12)
N4−Cu−N1	160.23(13)	N1−Cu−O3	92.03(11)

individual molecules are arranged in columns in opposed pairs, with phenyl rings arranged on either side of each column. The hydrogen bonds cross link the columns together. Pyridine inter-ring contacts are quite short (3.6−4.0 Å), indicating that π interactions are significant, and clearly contribute to the overall stability of the extended structure.

[Cu(PPOCCO-H)(NO_3)] (6). The structure of the mononuclear complex **6** is shown in Figure 8, and important bond distances and angles are listed in Table 7. The square-pyramidal copper(II) center coordinates to a tridentate N_3 ligand pocket, comprising pyridine, diazine, and oxime nitrogen atoms, which coordinate in the basal plane, thus creating adjacent five- and six-membered chelate rings. A fourth basal ligand site is occupied by nitrate oxygen O3. Bond distances to these donors are quite short (1.92−1.99 Å), indicating a quite strong ligand field. Oxygen O4 of the nitrate is poised above the axial position of the copper center (Cu−O4 2.531 Å) and can be considered as a pseudoaxial ligand, thus making the nitrate bidentate. The short equatorial bonds create a somewhat unusual distortion at the copper center, with an N1−Cu−N4 angle of 160.2° and a O3−Cu−N2 angle of 160.1° creating a slight tetrahedral

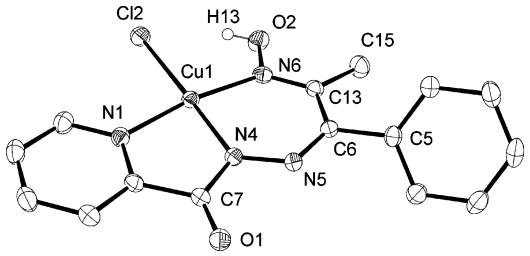

Figure 9. Structural representation for **7** (40% probability thermal ellipsoids).

Table 8. Distances (Å) and Angles (deg) for [Cu(PPOCCO-H)Cl] (**7**)

Cu1−N4	1.9209(17)	Cu1−N1	1.9891(18)
Cu1−N6	1.9742(17)	Cu1−Cl2	2.2680(6)
N4−Cu1−N6	89.15(7)	N4−Cu1−Cl2	178.64(6)
N4−Cu1−N1	83.01(7)	N6−Cu1−Cl2	92.21(5)
N6−Cu1−N1	171.44(8)	N1−Cu1−Cl2	95.63(5)

distortion, despite the axial contact. The carbonyl bond distance (C6−O1 1.231 Å) is short indicating double bond character and N2 as the site of ligand deprotonation. The ligand conformation changes dramatically on coordination, with nitrogen atoms N4 and N2 bonding to the metal. This causes a significant change in the relative orientation of the methyl group and the phenyl ring, which now are arranged in a pseudo-eclipsed conformation (C10−C7−C8−C9 torsional angle 18.5°). There are no significant intermolecular contacts.

[Cu(PPOCCO-H)Cl] (7). The structure of the mononuclear complex **7** is shown in Figure 9, and important bond distances and angles are listed in Table 8. The basal ligand coordination environment is the same as in **6**, with the fourth site at the square-planar copper center being occupied by a chloride ion. The maximum deviation of the donors in the coordination plane is 0.036(2) Å, with the copper ions displaced by 0.015(2) Å from the least-squares plane. A very short carbonyl distance (C7−O1 1.216(3) Å) and a very short Cu1−N4 distance (1.9209(17) Å) indicate N4 to be the site of ligand deprotonation. Again the methyl and phenyl groups are eclipsed (C5−C6−C13−C15 torsional angle 13.1°), and there are no significant intermolecular contacts.

Conformational Study on PPOCCO (5). The structure of the ligand PPOCCO (Figure 6) indicates that the preferred geometry involves an almost anti conformation of the phenyl and methyl groups around the oxime C−C bond. Density functional calculations (B3LYP/6-31G(d)) have been carried out for the keto and enol forms of both ligands, in both eclipsed and anti conformations, and the optimized structures are shown in Figure 10. The orientation of the pyridine rings in all cases involves the nitrogen pointing away from the adjacent phenyl or methyl group. This is different from the solid state structure in both cases, but is unlikely to be a significant perturbation on the overall energy differences. From the calculations performed, the keto tautomer is clearly the more stable of the possible structures. The rotational energy differences between the two forms ($\Delta E_{rot} = E_{eclipsed} - E_{anti}$) are given in Table 9. It is found in both cases that the anti conformer is more stable by ∼15−25 kJ mol^{-1}. Complexes **6** and **7** with PPOCCO exist with the ligand in

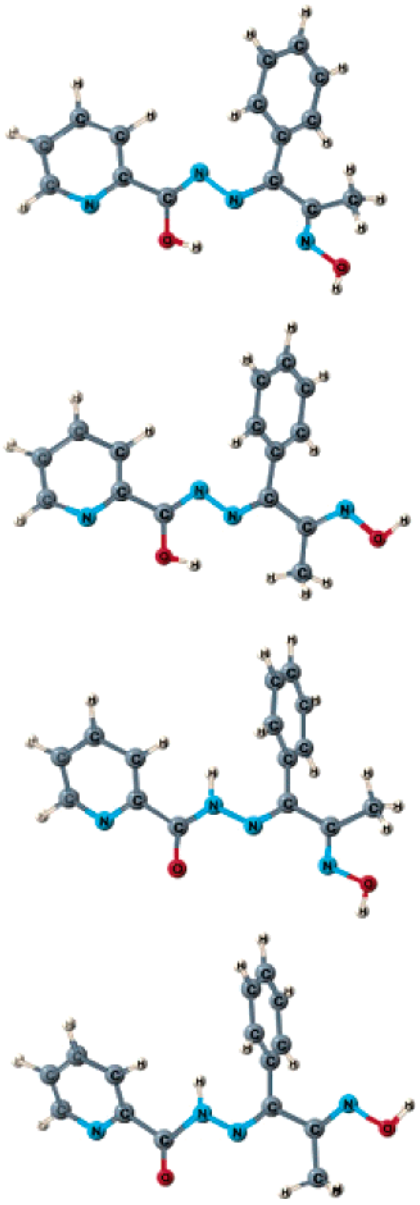

Figure 10. Optimized structures for the eclipsed and anti conformations of the keto and enol forms of the ligand PPOCCO **5**.

Table 9. Energies of Rotation for Keto and Enol Forms of PPOCCO

ligand	$E_{eclipsed}$ (hartree)	E_{anti} (hartree)	ΔE_{rot} (kJ/mol)
PPOCCO (keto)	−949.380 439 539	−949.390 521 574	26.47 ± 0.05
PPOCCO (enol)	−949.380 605 003	−949.385 549 269	12.98 ± 0.05

the eclipsed conformation, with pyridine, hydrazido, and oxime nitrogen atoms coordinating in the copper basal plane. Short C−O bond distances indicate that the ligand retains its keto form. Clearly the free ligand, with its preferred anti conformation, does not provide a suitable arrangement of donor atoms for coordination to the copper(II) ion, and despite the significant energy expenditure, the ligand conformation changes, with rotation about the N3−C7−C8−N4 framework, leading to the formation of a more suitable chelating N_3 donor grouping. A similar situation exists in the complex $[Cu_2(BDPAH\text{-}H)(NO_3)_2](NO_3)$,[11] where the ligand BDPAH takes advantage of its full donor capacity

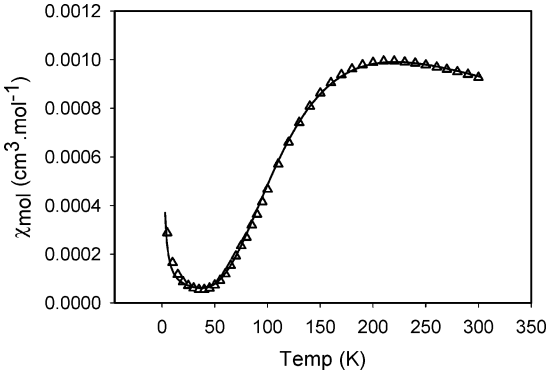

Figure 11. Magnetic data for **1**. The solid line is the best fit to eq 1, with $g = 2.13(1)$, $-2J = 246(1)$ cm^{-1}, $\rho = 0.0024$, $\Theta = -1.8$ K, and $N\alpha = 60 \times 10^{-6}$ cm^3·mol^{-1}.

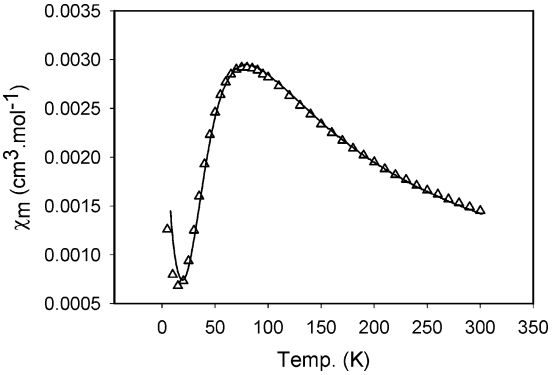

Figure 12. Magnetic data for **2**. The solid line is the best fit to eq 1, with $g = 2.22(2)$, $-2J = 91.5(5)$ cm^{-1}, $\rho = 0.024$, $\Theta = -1$ K, and $N\alpha = 65 \times 10^{-6}$ cm^3·mol^{-1}.

by orienting both ligand ends in a cis arrangement, such that the methyl groups are eclipsed.

Coordination Isomers. Compounds **1** and **2** involve ligands with the same structural framework, which normally self-assemble in the presence of transition metal ions, e.g. Mn(II), Co(II), Ni(II), and Cu(II), to produce [2 × 2] square or rectangular tetranuclear grid complexes.[3−10] This occurs when the accompanying anions have weak coordinating abilities (e.g. NO_3^-, ClO_4^-, BF_4^-) and do not compete successfully for metal coordination sites, which are then filled by nitrogen and oxygen donors from neighboring ligands, as the self-assembly process occurs. In the presence of more strongly coordinating anions, e.g. bromide, the situation changes and stronger ligand competition prevents grid formation, which in **1** and **2** leads to the formation of dinuclear complexes. In both cases there are three bromine ligands, which occupy equatorial and axial coordination positions. However the formation of two different coordination isomers with very similar ligands is difficult to explain but may be associated with the somewhat weaker donor capacity of pyrazine compared with pyridine, which is reflected in slightly longer Cu−N distances in **2**.

The very long Cu2−O1 bond in **2** (2.157(2) Å) is most unusual and is probably the result of the geometrical consequences of the "stretched" contiguous arrangement of three five-membered chelate rings, the "flat" nature of the coordinated ligand, and the inability of the ligand to twist through 90° at Cu2. Such a twist could possibly allow Cu2 to reorient its basal plane by 90°, thus allowing a perhaps more comfortable, longer axial coordination to O1. This is clearly what happens in the formation of the [$Cu_4(\mu$-O)$_4$] [2 × 2] grids, where the same constraints would apply. Here the equivalent Cu2−O1 bond ends up being an axial bond, because the strong in plane ligand field is established by N−O donor groupings from the second ligand, which would bind at ∼90° to the plane of the ligand in **2**.[3−10] The magnetic consequences are of course quite dramatic in the grids, because the alternating axial/equatorial bonding connections within the [$Cu_4(\mu$-O)$_4$] core lead to strict magnetic orbital orthogonality and intramolecular ferromagnetic behavior. The weak antiferromagnetic exchange in **2** (vide infra) clearly defines the nonorthogonality of the Cu1−O1−Cu2 connection but is also a signature of the consequences of a long Cu2−O1 bond.

Magnetic Properties. The variable-temperature magnetic properties of **1** are shown in Figure 11 as a plot of susceptibility/copper ion as a function of temperature. The characteristic maximum signals the presence of intramolecular antiferromagnetic exchange. The data were fitted to an exchange equation for two interacting spins ($H_{ex} = -2J\{S_1 \cdot S_2\}$; $S = 1/2$) (eq 1; ρ = mole fraction of paramagnetic impurity assumed to have a comparable molecular weight and g factor, Θ = Weiss-like temperature correction, $N\alpha$ = temperature-independent paramagnetism).

$$\chi_M = \frac{2Ng^2\beta^2}{k(T-\Theta)}\left[\frac{1}{(3+\exp(-2J/kT)}\right](1-\rho) + \left(\frac{Ng^2\beta^2}{4kT}\right)\rho + N\alpha \quad (1)$$

A good fit gave $g = 2.13(1)$, $-2J = 246(1)$ cm^{-1}, $\rho = 0.0024$, $\Theta = -1.8$ K, and $N\alpha = 60 \times 10^{-6}$ cm^3·mol^{-1} (Cu) ($10^2R = 0.67$; $R = [\Sigma(\chi_{obsd} - \chi_{calcd})^2/\Sigma\chi_{obs}^2]^{1/2}$). The solid line in Figure 11 was calculated with these parameters. The magnetic $d_{x^2-y^2}$ orbitals of the two copper(II) ions are connected through the N−N diazine bridge with a Cu−N−N−Cu torsional angle of 150.6°. This is a typical orientation of the copper magnetic orbitals for quite strong antiferromagnetic exchange,[1,2] where the calculated value for this torsional angle would be 152°, based on the generalized correlation between exchange and angle.[2] It is apparent that the presence of terminal bromine atoms does little to influence the exchange process, which is clearly dominated by the diazine bridge.

Compound **2** has a different "isomeric" bridging structure, with the two copper(II) ions bridged by the alkoxide type oxygen. The magnetic properties (Figure 12) again show a typical profile for intramolecular antiferromagnetic exchange, with a maximum in χ_{Cu} at ∼80 K. Analysis of the exchange using eq 1 gave $g = 2.22(2)$, $-2J = 91.5(5)$ cm^{-1}, $\rho = 0.024$, $\Theta = -1$ K, and $N\alpha = 65 \times 10^{-6}$ cm^3·mol^{-1} (Cu) ($10^2R = 1.2$). The solid line in Figure 12 was calculated with these parameters. The structure (Figure 2) reveals that the two copper square pyramids are connected basally via the alkoxide oxygen O1, with a C−O bond distance of 1.319

Table 10. Calculated Atomic Spin Populations for $[Cu_2(PZOAPZ\text{-}H)Br_3(H_2O)_2]$ (**2**)

atom	broken-symmetry singlet spin density
Cu1	−0.659 748
N1	−0.065 269
Br1	−0.181 975
O3	−0.041 839
O2	0.001 057
O1	−0.014 688
Cu2	0.661 779
N4	0.081 231
N7	0.060 298
Br3	0.107 157
Br2	0.040 686

Å, indicating the oxygen site to be deprotonated. The magnetic copper $d_{x^2-y^2}$ orbitals are therefore appropriately aligned for overlap via the oxygen bridge. The sum of the angles at O1 is 359.3°, indicating a trigonal planar oxygen bridge and optimal involvement of the oxygen "p" orbitals.

The exchange coupling constant is much smaller than would be expected on the basis of such a large Cu−O−Cu bridge angle (141.7°). Two systems with single oxygen bridges (OH) connecting two copper(II) centers with $d_{x^2-y^2}$ ground states via their basal planes, and very large bridge angles (132.2, 143.7°), have very large exchange integrals ($-2J = 820$, ∼1000 cm^{-1} respectively), typical for systems in this class.[29,30] Cu−O distances for these systems fall in the range 1.85−1.92 Å, much shorter than found in **2**. It is of interest to note that a related alkoxide-bridged dicopper(II) complex with a substituted 1,3-diaminopropanol ligand and a Cu−O−Cu bridge angle of 134.8° has a comparable and unexpectedly small coupling constant ($-2J = 111$ cm^{-1}), but one copper ion has close to trigonal bipyramidal geometry, thus creating a different orbital overlap situation.[31] Therefore, the only really significant structural features which could lead to such a dramatic reduction in exchange for **2** are the longer equatorial contacts from O1 and, in particular, the very long bond to Cu2 (2.157(2) Å), a distance which would be more typically associated with an axial contact. Another perhaps important feature is the "stretched" ligand framework itself, which in the μ-O bridging mode forces the copper ions to be at a certain distance and interposes the bridging oxygen atom between them. This extended dinuclear center undoubtedly results from the contiguous arrangement of the three five-membered chelate rings.

Density functional calculations on compound **2** predict an antiferromagnetic ground state with a singlet−triplet splitting ($-2J = 27$ cm^{-1}), somewhat smaller than the experimental value (91.5 cm^{-1}). However it is the same order of magnitude as the experimental value and very small compared with experimental values obtained for other compounds with similar Cu−O−Cu angles (vide supra). Since the calculations correctly predict the sign and magnitude of the coupling constant, it reinforces the fact that its relatively small magnitude is not simply an artifact of the fitting procedure

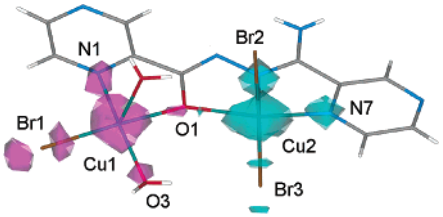

Figure 13. Spin density isosurface ($\rho = 0.005$ e/Bohr^3) for the broken-symmetry singlet state of **2** (see Table 9).

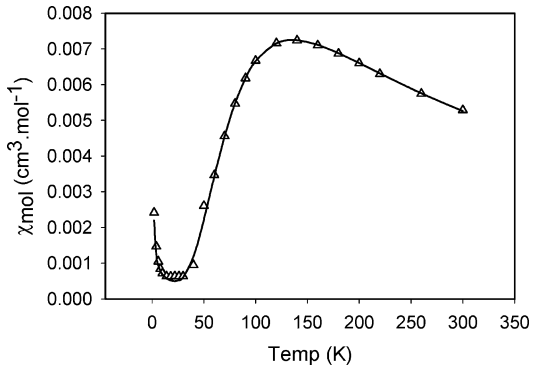

Figure 14. Magnetic data for **4**. The solid line is the best fit to eq 4, with $g = 2.239(4)$, $J_1 = -151(1)$ cm^{-1}, $J_2 = 0$ cm^{-1}, $\rho = 0.0003$, $\Theta = 0$ K, and $N\alpha = 310 \times 10^{-6}$ $cm^3 \cdot mol^{-1}$.

or sample purity. Rather, the weak antiferromagnetic coupling can be viewed as a result of two factors: poor overlap of the copper $d_{x^2-y^2}$ orbitals with those on the bridging oxygen atom and short-range spin delocalization due to the presence of the electronegative bromine atoms. The calculated spin density distribution for the broken-symmetry singlet state is given in Table 10, with a graphical representation shown in Figure 13. The very small spin density localized on the bridging oxygen is indicative of poor orbital overlap, which is consistent with the long copper−oxygen contacts in **2**, particularly Cu2−O1 (2.157(2) Å). Furthermore, there is significant spin delocalization toward the terminal bromide ligands via the copper atoms, which further serves to draw spin density away from the oxygen bridge. The degree of spin delocalization is similar to that reported previously for other Cu−Br complexes.[24]

Compound **3** shows a profile of magnetic moment versus temperature, which drops as temperature is lowered from 2.7 μ_B at 300 K to 1.25 μ_B at 20 K, followed by a slight increase at lower temperature, indicative of the presence of intramolecular antiferromagnetic exchange. Fitting of data to eq 1 was attempted, but it became apparent that the low-temperature regime could not be modeled successfully. An estimate of J was obtained by fitting the data above 50 K to eq 1, giving $g = 2.2$ and $-2J \sim = 300$ cm^{-1} (eq 1). A close examination of the bulk sample of **3** reveals the presence of noncrystalline impurities, which are estimated as a 25% Curie-like paramagnetic contribution in the magnetic analysis. The estimated coupling constant is consistent with the almost trans arrangement of the copper basal planes in **3** (Cu−N−N−Cu 162°).[1,2]

Compound **4** shows a maximum in molar susceptibility at 130 K (Figure 14), indicating the presence of intramo-

(29) Burk, P. L.; Osborne, J. A.; Youinou, M.-T.; Agnus, Y.; Louis, R.; Weiss, R. *J. Am. Chem. Soc.* **1981**, *103*, 1273.
(30) Coughlin, P. K.; Lippard, S. J. *J. Am. Chem. Soc.* **1981**, *103*, 3228.
(31) Arif, H.; Funahashi Y.; Jitsukawa K.; Masuda H. *J. Chem. Soc., Dalton Trans.* **2003**, 2115.

lecular antiferromagnetic exchange. The magnetic data have been fitted to an exchange expression based on an exchange Hamiltonian (eq 2) for a rectangle of four copper(II) ions ($S = 1/2$), with two different J values, appropriate to the alkoxy and diazine bridges. The total (S') spin quantum numbers and their energies were calculated using normal vector addition principles and substituted into the Van Vleck eq 3 within the software package MAGMUN4.0.[32] Corrections were made for paramagnetic impurity fraction (ρ), intermolecular exchange effects with a Weiss-like Θ factor, and temperature-independent paramagnetism (eqs 3 and 4). An excellent fit gave $g = 2.239(4)$, $J_1 = -151(1)$ cm^{-1}, $J_2 = 0$ cm^{-1}, $\rho = 0.003$, $\Theta = 0$ K, and $N\alpha = 310 \times 10^{-6}$ cm^3·mol^{-1}, $10^2R = 0.65$. The solid line in Figure 14 was calculated with these parameters. The fact that the fitting gives $J_2 = 0$ cm^{-1} is clearly consistent with the orthogonal alkoxide bridging arrangement. The J_1 value is entirely consistent with the large Cu−N−N−Cu torsional angle (159.2°) at the diazine bridge and the correlations involving this angle and exchange integral for a series of dinuclear copper(II) compexes.[1,2] This complex can be considered as an essentially isolated pair of antiferromagnetically coupled dinuclear species.

$$H_{ex} = -J_1\{S_1 \cdot S_2 + S_3 \cdot S_4\} - J_2\{S_2 \cdot S_3 + S_1 \cdot S_4\} \quad (2)$$

$$\chi_{M'} = \frac{N\beta^2 g^2}{3k(T-\Theta)} \frac{\Sigma S'(S'+1)(2S'+1)e^{-E(S')/kT}}{\Sigma(2S'+1)e^{-E(S')/kT}} \quad (3)$$

$$\chi_M = \chi_{M'}(1-\rho) + \frac{S(S+1)N\beta^2 g^2 \rho}{3kT} + N\alpha \quad (4)$$

Conclusion

Two structurally isomeric dicopper(II) complexes exist with a pair of closely related ligands, involving μ-N−N and μ-O bridging groups. The alkoxide (μ-O) bridged complex exhibits anomalously low exchange coupling, which is attributed to poor magnetic orbital overlap via the oxygen bridge as a result of an unusually long Cu−O distance. DFT calculations based on the X-ray structure have been used to model the exchange situation and lead to an exchange integral comparable with the experimentally determined value.

Acknowledgment. We thank the NSERC (Natural Sciences and Engineering Research Council of Canada), the Research Council of Norway (H.G.), and the EPSRC (A.E.G., C.W., J.A.K.H.) for financial support. Dr. R. McDonald, University of Alberta, is acknowledged for structural data on compound **4**. We thank Professor Santiago Alvarez (University of Barcelona) for helpful comments and suggestions.

Supporting Information Available: X-ray crystallographic data in CIF format for **1**−**7**. This material is available free of charge via the Internet at http://pubs.acs.org. Crystallographic data in CIF format have also been deposited with the Cambridge Crystallographic Data Center, CCDC Nos. 232797−232803. Copies of this information may be obtained free of charge from the Director, CCDC, 12 Union Road, Cambridge, CB2 1EZ, UK (fax +44-1223-336033; e-mail deposit@ccdc.cam.ac.uk; http://www.ccdc.cam.ac.uk).

IC040036I

(32) MAGMUN4.0 is available free of charge. It has been developed by Dr. Zhiqiang Xu (Memorial University) in collaboration with Prof. L. K. Thompson (lthomp@mun.ca) and Dr. O. Waldmann (oliver.waldmann@iac.unibe.ch). We do not distribute the source codes. The programs may be used for scientific purposes only, and economic utilization is not allowed.